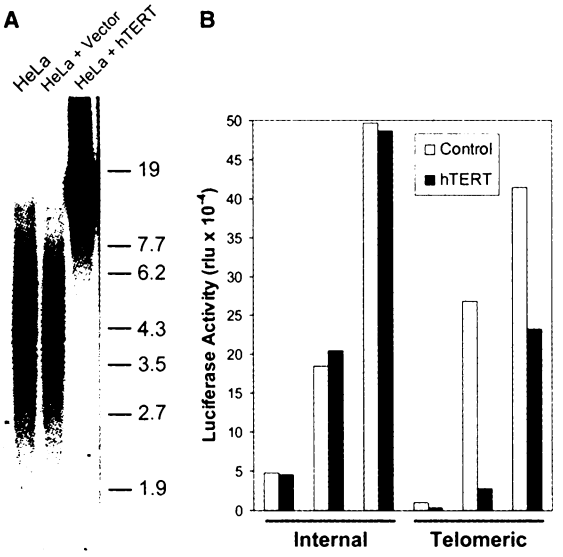

Fig. 3. Silencing in telomeric clones is enhanced by an increase in telomere length. **(A)** Infection of HeLa cells with an hTERT-encoding retrovirus causes telomere elongation, as demonstrated by terminal restriction fragment analysis. Mean telomere length increased from approximately 5 kb to almost 14 kb. Genomic DNA was digested with six restriction enzymes to degrade nonrepetitive sequences. Samples were then separated on a 0.7% agarose gel and probed with an oligonucleotide complementary to telomere repeats. Markers shown are λ *Sty* (in kilobases). **(B)** Telomeric clones infected with hTERT express 2 to 10 times lower levels of luciferase activity as compared to control, vector-only infections. Internal clones having comparable initial values retain full expression of the luciferase reporter after infection with hTERT.

telomeric DNA (*17*). It is possible that the extra telomeric sequences in ALT cells are titrating out factors essential for TPE, as has been observed in yeast (*18*), so that ALT cells might not exhibit TPE. Another report may have failed to identify TPE, because the healed telomere appears to have been extremely short and/or because it was located >50 kb from the nearest gene that could be examined (*9*). In at least one case, data consistent with a very mild mammalian TPE have been described (*19*), and the insertion of telomere repeats into an intron of the *APRT* gene of Chinese hamster cells was shown to cause a twofold reduction in the mRNA level (*20*).

A number of proteins have been reported to change in expression level as a function of the replicative age of the cell (*21*, *22*). The existence of TPE in mammalian cells raises the possibility that some presenescent changes could be "programmed" by the progressive shortening of telomeres with ongoing cell division, leading to altered patterns of gene expression that might affect both cell and organ function. It will be important to identify endogenous genes whose expression is influenced by telomere length in order to determine whether TPE actually influences the physiology of aging or cancer.

References and Notes

1. C. B. Harley, *Mutat. Res.* **256**, 271 (1991).
2. E. Hara, H. Tsurui, A. Shinozaki, S. Nakada, K. Oda, *Biochem. Biophys. Res. Commun.* **179**, 528 (1991).
3. J. W. Shay, O. M. Pereira-Smith, W. E. Wright, *Exp. Cell Res.* **196**, 33 (1991).
4. D. E. Gottschling, O. M. Aparicio, B. L. Billington, V. A. Zakian, *Cell* **63**, 751 (1990).
5. H. Renauld *et al.*, *Genes Dev.* **7**, 1133 (1993).
6. G. Kyrion, K. Liu, C. Liu, A. J. Lustig, *Genes Dev.* **7**, 1146 (1993).
7. W. E. Wright, J. W. Shay, *Trends Genet.* **8**, 193 (1992).
8. C. N. Sprung, L. Sabatier, J. P. Murnane, *Nucleic Acids Res.* **24**, 4336 (1996).
9. R. Ofir, A. C. Wong, H. E. McDermid, K. L. Skorecki, S. Selig, *Proc. Natl. Acad. Sci. U.S.A.* **96**, 11434 (1999).
10. R. A. Bayne *et al.*, *Hum. Mol. Genet.* **3**, 539 (1994).
11. Supplementary Web material is available on *Science* Online at www.sciencemag.org/cgi/content/full/292/5524/2075/DC1
12. J. P. Hanish, J. L. Yanowitz, T. de Lange, *Proc. Natl. Acad. Sci. U.S.A.* **91**, 8861 (1994).
13. P. A. Marks, V. M. Richon, R. A. Rifkind, *J. Natl. Cancer Inst.* **92**, 1210 (2000).
14. T. Yamano *et al.*, *Mol. Ther.* **1**, 574 (2000).
15. J. A. Baur, J. W. Shay, W. E. Wright, unpublished data.
16. P. A. McChesney, D. L. Aisner, B. C. Frank, W. E. Wright, J. W. Shay, *Mol. Cell. Biol. Res. Commun.* **3**, 312 (2000).
17. T. M. Bryan, L. Marusic, S. Bacchetti, M. Namba, R. R. Reddel, *Hum. Mol. Genet.* **6**, 921 (1997).
18. E. A. Wiley, V. A. Zakian, *Genetics* **139**, 67 (1995).
19. H. Cooke, in *Telomeres*, E. Blackburn, Ed. (Cold Spring Harbor Laboratory Press, Plainview, NY, 1995), pp. 238–239.
20. A. E. Kilburn, M. J. Shea, R. G. Sargent, J. H. Wilson, *Mol. Cell. Biol.* **21**, 126 (2001).
21. M. Tresini, R. J. Pignolo, R. G. Allen, V. J. Cristofalo, *J. Cell Physiol.* **179**, 11 (1999).
22. L. Hayflick, in *Annual Review of Gerontology and Geriatrics*, C. Eisdorf, Ed. (Springer, New York, 1980), pp. 26–67.

23. W. E. Wright, V. M. Tesmer, K. E. Huffman, S. D. Levene, J. W. Shay, *Genes Dev.* **11**, 2801 (1997).
24. We thank C. Iucu for excellent technical support. Funding for this work was provided by the Ellison Medical Foundation (J.A.B. and J.W.S.), U.S. Department of Defense grant BC000422 (J.A.B. and J.W.S.), NIH grant AG07792 (W.E.W.), and the Geron Corporation, Menlo Park, CA.

7 March 2001; accepted 8 May 2001

Requirement of *CHROMOMETHYLASE3* for Maintenance of CpXpG Methylation

Anders M. Lindroth,[1*] Xiaofeng Cao,[1*] James P. Jackson,[1*] Daniel Zilberman,[1] Claire M. McCallum,[3] Steven Henikoff,[2,3] Steven E. Jacobsen[1†]

Epigenetic silenced alleles of the *Arabidopsis SUPERMAN* locus (the *clark kent* alleles) are associated with dense hypermethylation at noncanonical cytosines (CpXpG and asymmetric sites, where X = A, T, C, or G). A genetic screen for suppressors of a hypermethylated *clark kent* mutant identified nine loss-of-function alleles of *CHROMOMETHYLASE3* (*CMT3*), a novel cytosine methyltransferase homolog. These *cmt3* mutants display a wild-type morphology but exhibit decreased CpXpG methylation of the *SUP* gene and of other sequences throughout the genome. They also show reactivated expression of endogenous retrotransposon sequences. These results show that a non-CpG DNA methyltransferase is responsible for maintaining epigenetic gene silencing.

Cytosine methylation plays a major role in determining the epigenetic expression state of eukaryotic genes. This methylation is most often found at the symmetrical dinucleotide CG (or CpG sites). CpG methylation is maintained by the well-studied DNMT1 subfamily of methyltransferases, which includes *Arabidopsis* MET1 (*1–3*). Methylation at sites other than CpG is also found in many organisms (*4*), but the mechanism by which this methylation is maintained is poorly understood. *Arabidopsis* can tolerate major disruptions in DNA methylation (*2, 3, 5*), making it useful for genetic analysis of methylation pattern-

[1]Department of Molecular, Cell and Developmental Biology, University of California, Los Angeles, CA 90095, USA. [2]Howard Hughes Medical Institute, [3]Fred Hutchinson Cancer Research Center, Seattle, WA 98109, USA.

*These authors contributed equally to this work.
†To whom correspondence should be addressed. E-mail: jacobsen@ucla.edu

ing. For unknown reasons, the floral development gene *SUPERMAN* (*SUP*) becomes densely hypermethylated and silenced in several mutants that display genome-wide hypomethylation. It occurs in plants expressing antisense RNA to the *MET1* gene (*6*), in a *met1* loss-of-function mutant (previously called *ddm2*) (*7, 8*), and in *ddm1* mutants (*5, 7*). In this way, *SUP* hypermethylation resembles a phenomenon observed in cancer cells, where genome-wide loss of methylation is frequently associated with hypermethylation and silencing of particular tumor suppressor genes (*9*).

SUP hypermethylation causes a floral phenotype similar to that of known loss-of-function *sup* mutants: an increased number of stamens and a defective gynoecium (female reproductive structure) (Fig. 1A). These hypermethylated *SUP* alleles (called the *clark kent* alleles) are recessive and heritable. They are associated with dense methylation at CpG sites, at CpXpG sites (X = A, T, C, or G), and at asymmetric sites (those cytosines not present in the symmetric CpG or CpXpG contexts). *clark kent* alleles that arise in an antisense-*MET1* background or in the *met1* mutant lack most CpG methylation but maintain the other types (*6, 8*), showing that non-CpG methylation is critical for the maintenance of *SUP* gene silencing.

To identify loci important for maintenance of methylation and silencing of *SUP*, we performed a mutant screen for suppressors of a nonreverting *clark kent* allele, *clk-st*, created by introducing an additional *SUP* locus into *clark kent-3* plants (*6, 10*). *clk-st* seeds were mutagenized with ethylmethane sulfonate, and individual M2 families were screened for mutations that derepress *SUP* gene silencing, leading to plants with a wild-type floral phenotype (*10*). Sixteen independent recessive mutants were recovered and five were chosen for initial study. Of these, four completely reverted the *clark kent* phenotype to yield wild-type flowers (Fig. 1B), and one displayed partial reversion. Each of the five mutants failed to complement any of the others, indicating that they are loss-of-function alleles of the same gene (*10*).

One of these mutations was mapped to the bottom of chromosome I (*10*), near the *CHROMOMETHYLASE3* (*CMT3*) gene. *CMT3* encodes a putative cytosine methyltransferase containing a chromodomain and a bromo-adjacent homology (BAH) domain (*11–13*). We crossed one of the strong suppressors to *cmt3-2*, a nonsense allele of *CMT3* isolated previously (*13*). These mutants failed to complement (*10*), showing that all five suppressor mutants are alleles of *CMT3*, here designated *cmt3-3* (the partial suppressor), *cmt3-4*, *cmt3-5*, *cmt3-6*, and *cmt3-7*.

The molecular lesions in the *cmt3* mutants were identified by sequencing 5021 base pairs (bp) of the *CMT3* gene from each homozygous mutant line. A single C/G to T/A transition mutation was found in each mutant, in every case altering the coding region of *CMT3* (Fig. 1C) (GenBank accession number AF364174). We used the DNA polymorphisms created by the *cmt3-4*, *-5*, *-6*, and *-7* mutations to generate molecular markers, and we found that these markers perfectly cosegregated with the suppressor mutant phenotypes (*10*). The *cmt3-5* and *cmt3-7* alleles contain stop codons terminating CMT3 after 95 or 27 amino acids, respectively, and thus they likely represent null alleles. The *cmt3-3*, *cmt3-4*, and *cmt3-6* alleles are missense mutations within the methyltransferase segment of *CMT3* (Fig. 1C) (*14*). We identified four additional *cmt3* alleles by sequencing the *CMT3* gene from each of our remaining 11 mutants (Fig. 1C). *cmt3-9* and *cmt3-11* are phenotypically strong suppressors and contain nonsense mutations; *cmt3-8* and *cmt3-10* are phenotypically weak alleles and contain missense mutations in the methyltransferase segment. Thus, 9 of the 16 mutants isolated from our screen are alleles of *CMT3*.

We used bisulfite genomic sequencing (*10*) to determine the effect of *CMT3* on methylation patterning. We compared the methylation profiles of three genotypes: line *clk-st*, *cmt3-7* in the *clk-st* background, and a previously described *met1* mutant line that had developed a *clark kent* phenotype (*10*). We cloned and sequenced individual polymerase chain reaction (PCR) products from the *SUP* gene, the long terminal repeat (LTR) of a pericentromeric Athila retrotransposon (*15*), and the 180-bp centromeric repeat sequence (Fig. 2) (*10*). The *cmt3-7* mutant showed a nearly complete loss of CpXpG methylation in all sequences tested, but it retained the majority of CpG methylation. In contrast, *met1* showed a marked reduction in CpG methylation but had little effect on the level of CpXpG methylation. *cmt3-7* displayed variable effects on asymmetric methylation, ranging from no reduction to nearly complete loss at the 5′ end of the *SUP* locus (Fig. 2). In this region, asymmetric methylation may depend on the presence of CpXpG methylation. Using direct sequencing of PCR products of bisulfite-treated DNA from *SUP* and the Athila LTR, we found that three additional *cmt3* alleles (*cmt3-4*, *cmt3-5*, and *cmt3-6*) showed a pattern of methylation similar to that of *cmt3-7*.

We analyzed the effect of *cmt3-7* on meth-

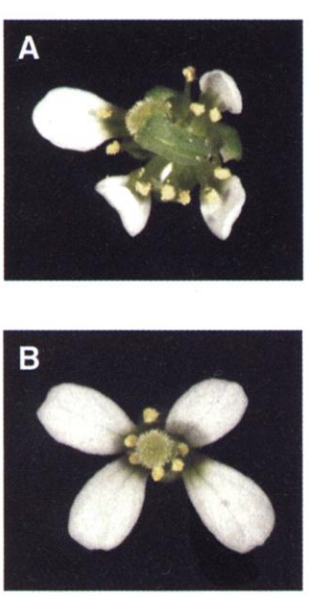

C

```
                          cmt3-7 R28 to stop
1   MAPKRKRPATKDDTTKSIPKPKKRAPKRAKTVKEEPVTVVEEGEKHVARFLDEPIPESEAKSTWPDRYKP
                        cmt3-5 R96 to stop                BAH domain
71  IEVQPPKASSRKKTKDDEKVEIIRARCHYRRAIVDERQIYELNDDAYVQSGEGKDPFICKIIEMFEGVNG

141 KLYFTARWFYRPSDTVMKEFEILINKKRVFFSEIQDTNELGLLEKKLNILMIPLNENTKETIPATENCDF

211 FCDMNYFLPYDTFEAIQQETMMAISESSTISSDTDIREGAAAISEIGECSQETEGQKEATLLDLYSGCGA
                                                                  I  *  * *
281 MSTGLCMGAQLSGLNLVTKWAVDMNAHACKSLQHNHPETNVRNMTAEDFLFLLKEWEKLCIHFSLRNSPN

                                  Chromodomain      cmt3-9 W419 to stop
351 SEEYANLHGLNNVEDNEDVSEESENEDDGEVFTVDKIVGISFGVPKKLLKRGLYLKVRWLNYDDSHDTWE

                                                cmt3-10 R470 to K
421 PIEGLSNCRGKIGEFVKLGYKSGILPLPGGVDVVCGGPPCQGISGHNRFRNLLDPLEDQKNKQLLVYMNI
                                        IV  * ***  *

                                                cmt3-6 G541 to E
491 VEYLKPKFVLMENVVDMLKMAKGYLARFAVGRLLQMNYQVRNGMMAAGAYGLAQFRLRFFLWGALPSEII
      VI *     ***                                VIII  *  * * *

561 PQFPLPTHDLVHRGNIVKEFQGNIVAYDEGHTVKLADKLLLKDVISDLPAVANSEKRDEITYDKDPTTPF

631 QKFIRLRKDEASGSQSKSKSKKHVLYDHHPLNLNINDYERVCQVPKRKGANFRDFPGVIVGPGNVVKLEE

  cmt3-4 G724 to E cmt3-11 P729 to stop cmt3-8 S763 to F cmt3-3 R769 to K
701 GKERVKLESGKTLVPDYALTYVDGKSCKPFGRLWWDEIVPTVVTRAEPHNQVIIHPEQNRVLSIRENARL
                                                                  IX *  *

771 QGFPDDYKLFGPPKQKYIQVGNAVAVPVAKALGYALGTAFQGLAVGKDPLIILPEGFAFMKPTLPSELA
                                X ** *
```

Fig. 1. *CMT3* mutations. (**A**) *clk-st* flower containing 10 stamens and three incompletely fused carpels. (**B**) Flower from the *cmt3-7* suppressor mutant, showing the normal number of six stamens and a normal gynoecium consisting of two fused carpels. (**C**) The CMT3 protein sequence determined from the Ler ecotype. Residues constituting the BAH (bromo-adjacent homology) domain and the chromodomain are underlined. Conserved methyltransferase catalytic motifs I, IV, VI, and VIII–X are marked. Asterisks denote highly conserved amino acids present in each motif (*14*), derived from alignments with the bacterial methylase Hha I. Residues mutated in the *cmt3* mutants are in boldface. Single-letter abbreviations for amino acid residues are as follows: A, Ala; C, Cys; D, Asp; E, Glu; F, Phe; G, Gly; H, His; I, Ile; K, Lys; L, Leu; M, Met; N, Asn; P, Pro; Q, Gln; R, Arg; S, Ser; T, Thr; V, Val; W, Trp; and Y, Tyr.

ylation within the direct repeats present in the promoter of the *FWA* locus. These repeats were previously found to be methylated predominantly at CpG sites in wild-type plants, causing *FWA* expression to be silenced (*16*). When this methylation is lost, either spontaneously or in the *ddm1* mutant, the *FWA* gene is overexpressed, causing a dominant late-flowering phenotype (*16*). Using direct sequencing of PCR products from bisulfite-treated genomic DNA, we found that the CpG methylation pattern was similar in line *clk-st* and in *cmt3-7*. However, this CpG methylation was lost in a *met1* mutant line that had developed an *fwa* late-flowering mutant phenotype. Furthermore, no *fwa*-like late-flowering phenotypes have been observed in any of the *cmt3* alleles, even after several generations of inbreeding. Thus, the *cmt3* mutations do not appear to affect the CpG methylation or gene silencing at the *FWA* locus.

To determine whether loss of CpXpG methylation in the *cmt3* mutants is genome-wide, we performed Southern blot analysis with methylation-sensitive restriction enzymes. Both *cmt3-5* and *cmt3-7* showed an increased level of enzyme digestion at the Athila LTR sequences with the enzymes Eco RII [which is inhibited by methylation of the inner cytosine within its recognition site CC(A/T)GG] and Msp I (inhibited by methylation of the outer cytosine of its recognition site CCGG). However, the *cmt3* mutants showed a level of digestion equal to the wild type with the enzymes Hpa II and Hha I, which are inhibited by CpG methylation in their recognition sites (Fig. 3). Using similar restriction enzyme analyses, we found that *cmt3* mutants exhibit decreased CpXpG methylation, but not CpG methylation, at the centromeric 180-bp repeat sequence (*5*) and at the Ta3 retrotransposon sequence (*17*). We also analyzed *cmt3-2*, a strong *CMT3* allele in the Nossen genetic background (*13*). This allele showed increased digestion with Msp I, but not with Hpa II, using both a 180-bp centromeric repeat probe (Fig. 3) and an *Arabidopsis* ribosomal DNA probe (*5*). In summary, the *cmt3* mutants showed decreased CpXpG methylation at all sequences examined.

We tested the role of *CMT3* in the silencing of endogenous *Arabidopsis* retrotransposons. We analyzed the expression of an Athila sequence that was previously shown to be heavily methylated and silenced in wild-type plants but transcriptionally activated in several *Arabidopsis* silencing mutants, including *met1* (*18*). Figure 4A shows that 2.5-kb and 1.2-kb Athila-related transcripts are indeed activated in the *cmt3-7* mutant line. These transcripts are similar in size to those activated by other silencing mutants (*18*). We also tested for expression of the Ta3 element, a copia-like retrotransposon previously found to be transcriptionally silent in both the wild type and the *ddm1* mutant (*17, 19*). A 5.3-kb transcript was easily detected in *cmt3-7*, but no expression was observed in the wild-type line *clk-st* (Fig. 4B). Using similar analyses, we did not see activation of two additional retrotransposons: Evelknievel (*11*), or Tar17, which was previously shown to be reactivated in the *ddm1* mutant (*19*). Together, these results demonstrate that *CMT3* is required for maintaining gene silencing at a subset of retrotransposon sequences.

Our results suggest that CMT3 is specific for CpXpG methylation—a specificity different from that of the DNMT1/MET1 class of methyltransferases. Because *cmt3* mutants show a loss of CpXpG methylation in a background that is wild type for *MET1*, MET1 cannot substitute for the function of CMT3 at these sites. This corroborates earlier observations of distinct CpG and CpXpG methylases that could be purified from plant extracts (*20*), and is consistent with observations (*21*) suggesting that a mutation of a maize *CMT3* homolog, *Zmet2*, causes a specific reduction in CpXpG methylation (*22*). *CMT* genes have thus far only been found in the plant kingdom (*23*), which agrees well with the observation that plants have a much higher incidence of CpXpG methylation than do other organisms such as mammals (*4*).

The differential reactivation of gene expression observed in the *cmt3* mutants suggests a model where different loci may depend preferentially on either CpXpG or CpG methylation as the main mechanism of gene silencing. For

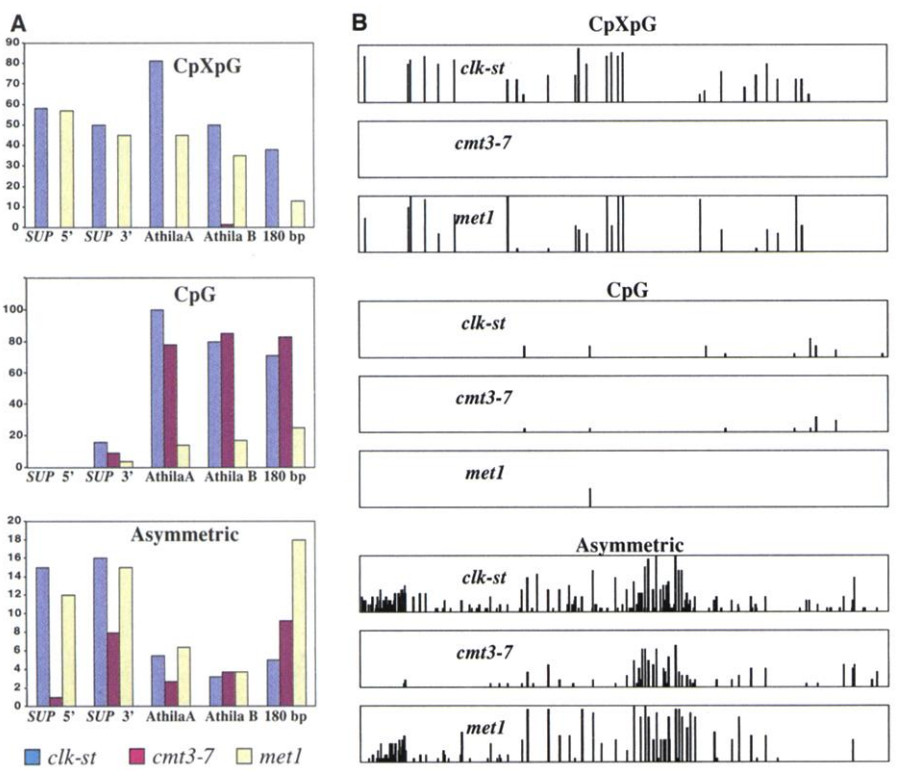

Fig. 2. Methylation profiles of the *cmt3* and *met1* mutants. (**A**) Histograms represent the percentage of methylated cytosines found in different contexts in *clk-st* (blue), *cmt3-7* (red), or *met1* (yellow), derived from cloned PCR products of bisulfite-treated genomic DNA of five regions: the 5′ and 3′ regions of *SUP*, two regions (A and B) of the Athila LTR, or the 180-bp centromeric repeat. (**B**) Diagram represents a 1028-nucleotide region of the top strand of the *SUP* gene, with the height of each bar representing the frequency of methylation found in different sequence contexts, within 15 cloned PCR products. For details of these experiments, see (*10*).

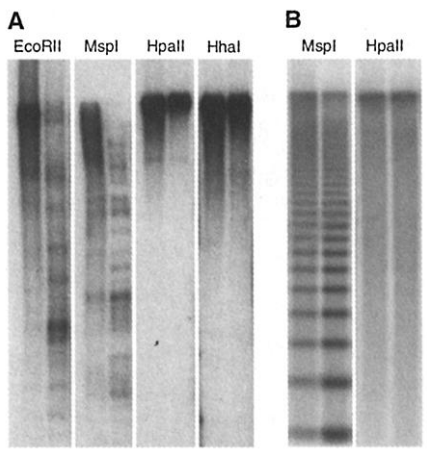

Fig. 3. Southern blot analysis of *cmt3* mutants. (**A**) Genomic DNA of wild-type Ler (left) and *cmt3-5* (right) digested with the indicated restriction enzyme. Blot was probed with an Athila LTR probe (*10*). (**B**) Genomic DNA of wild-type Nossen (left) and *cmt3-2* (right) digested with the indicated restriction enzyme. Blot was probed with a 180-bp centromeric repeat probe (*5*). Note the more intense lower molecular weight bands in the Msp I digest of the *cmt3-2* mutant.

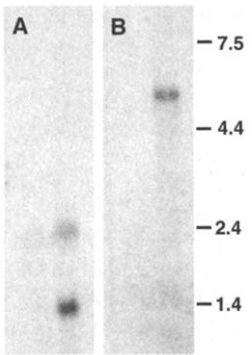

Fig. 4. Retrotransposon expression in *cmt3* mutants. Blots containing 40 μg of total RNA from whole shoots of line *clk-st* (left) or *cmt3-7* (right) were hybridized with either an Athila probe (**A**) or a Ta3 probe (**B**) (*10*). The positions of molecular size markers (in kilobases) are indicated.

instance, *SUP* and the Ta3 retrotransposon appear to depend more heavily on CpXpG methylation, whereas FWA and possibly Tar17 rely more on CpG methylation. Athila sequences require both types of methylation, because Athila-related transcripts are activated in both *cmt3* and *met1* mutants.

Despite a nearly complete loss of genomic CpXpG methylation, null *cmt3* mutants are morphologically normal, even after five generations of inbreeding. In contrast, *met1* mutants exhibit severe developmental abnormalities (*3*, *7*). One explanation for this is that CpXpG and CpG methylation may act in a partially redundant fashion to silence most genes. Viability despite severe loss of genomic methylation makes *Arabidopsis* an ideal model system for elucidating the roles of DNA methylation in epigenetic and developmental processes.

References and Notes

1. T. Bestor, A. Laudano, R. Mattaliano, V. Ingram, *J. Mol. Biol.* **203**, 971 (1988).
2. M. J. Ronemus, M. Galbiati, C. Ticknor, J. Chen, S. L. Dellaporta, *Science* **273**, 654 (1996).
3. E. J. Finnegan, W. J. Peacock, E. S. Dennis, *Proc. Natl. Acad. Sci. U.S.A.* **93**, 8449 (1996).
4. Y. Gruenbaum, T. Naveh-Many, H. Cedar, A. Razin, *Nature* **292**, 860 (1981).
5. A. Vongs, T. Kakutani, R. A. Martienssen, E. J. Richards, *Science* **260**, 1926 (1993).
6. S. E. Jacobsen, E. M. Meyerowitz, *Science* **277**, 1100 (1997).
7. S. E. Jacobsen, H. Sakai, E. J. Finnegan, X. Cao, E. M. Meyerowitz, *Curr. Biol.* **10**, 179 (2000).
8. N. Kishimoto *et al.*, *Plant Mol. Biol.*, in press.
9. S. B. Baylin, J. G. Herman, *Trends Genet.* **16**, 168 (2000).
10. For supplemental data and methods, see *Science* Online (www.sciencemag.org/cgi/content/full/1059745/DC1).
11. S. Henikoff, L. Comai, *Genetics* **149**, 307 (1998).
12. I. Callebaut, J. C. Courvalin, J. P. Mornon, *FEBS Lett.* **446**, 189 (1999).
13. C. M. McCallum, L. Comai, E. A. Greene, S. Henikoff, *Nature Biotechnol.* **18**, 455 (2000).
14. X. Cheng, *Annu. Rev. Biophys. Biomol. Struct.* **24**, 293 (1995).
15. T. Pelissier, S. Tutois, S. Tourmente, J. M. Deragon, G. Picard, *Genetica* **97**, 141 (1996).
16. W. J. Soppe *et al.*, *Mol. Cell* **6**, 791 (2000).
17. A. Konieczny, D. F. Voytas, M. P. Cummings, F. M. Ausubel, *Genetics* **127**, 801 (1991).
18. A. Steimer *et al.*, *Plant Cell* **12**, 1165 (2000).
19. H. Hirochika, H. Okamoto, T. Kakutani, *Plant Cell* **12**, 357 (2000).
20. S. Pradhan, R. L. Adams, *Plant J.* **7**, 471 (1995).
21. C. M. Papa, N. M. Springer, M. G. Muszynski, S. M. Kaeppler, unpublished data.
22. E. J. Finnegan, K. A. Kovac, *Plant Mol. Biol.* **43**, 189 (2000).
23. T. M. Rose *et al.*, *Nucleic Acids Res.* **26**, 1628 (1998).

24. Supported by NIH grant GM60398, a Beckman Young Investigator grant, a Searle Scholar award (S.E.J.), NIH training grants GM07104 (J.P.J.) and GM07185 (D.Z.), and NIH grant GM29009 (S.H.). We thank C. Hyun, M. Huang, L. Cahoon, and H. Le for technical assistance; S. Kaeppler and N. Springer for helpful discussions; and E. Richards for the *met1* mutant.

9 February 2001; accepted 23 April 2001
Published online 10 May 2001;
10.1126/science.1059745
Include this information when citing this paper.

Ordering Genes in a Flagella Pathway by Analysis of Expression Kinetics from Living Bacteria

S. Kalir,[1] J. McClure,[3] K. Pabbaraju,[3] C. Southward,[3] M. Ronen,[1] S. Leibler,[4] M. G. Surette,[3] U. Alon[1,2]*

The recent advances in large-scale monitoring of gene expression raise the challenge of mapping systems on the basis of kinetic expression data in living cells. To address this, we measured promoter activity in the flagellar system of *Escherichia coli* at high accuracy and temporal resolution by means of reporter plasmids. The genes in the pathway were ordered by analysis algorithms without dependence on mutant strains. The observed temporal program of transcription was much more detailed than was previously thought and was associated with multiple steps of flagella assembly.

Under the proper conditions, the bacterium *E. coli* synthesizes multiple flagella, which allow it to swim rapidly. Classical genetics showed that the 14 flagella operons are arranged in a regulatory cascade of three classes (*1*–*5*) (Fig. 1). The class 1 operon encodes the transcriptional activator of class 2 operons. Class 2 genes include structural components of a rotary motor called the basal body–hook structure, as well as the transcriptional activator for class 3 operons. Class 3 includes flagellar filament structural genes and the chemotaxis signal transduction system that directs the cells' motion. A checkpoint mechanism ensures that class 3 genes are not transcribed before functional basal body–hook structures are completed (Fig. 1).

Here, we developed a system for real-time monitoring of the transcriptional activation of the flagellar operons by means of a panel of 14 reporter plasmids in which green fluorescent protein (GFP) (*6*) is under the control of one of the flagellar promoters (*7*). This allowed us to extend previous timing studies that depended on lacZ fusions to up to four operons (*8*, *9*). Use of GFP eliminates the need for cell lysis required for lacZ and DNA microarray studies (*10*–*13*). Therefore, the present system makes it possible to measure accurately continuous time courses from living cells grown in a multiwell

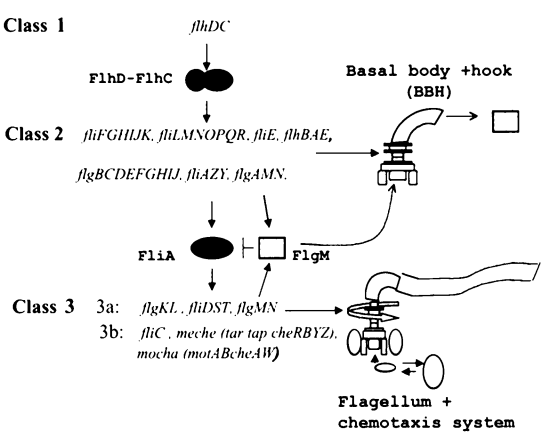

Fig. 1. The genetically defined hierarchy of flagellar operons in *Escherichia coli* (*1*, *2*). The master regulator FlhDC turns on class 2 genes, one of which, FliA, turns on class 3 genes. A checkpoint ensures that class 3 genes are not turned on until basal body–hook structures (BBH) are completed. This is implemented by FlgM, which binds and inhibits FliA. When BBH are completed, they export FlgM out of the cell, leaving FliA free to activate the class 3 operons (*9*, *27*, *28*). Note that *flgM* is transcribed from both a class 2 (*flgAMN*) and a class 3 (*flgMN*) promoter.